

Atmospheric Chemistry Signatures of an Equatorially Symmetric Matsuno–Gill Circulation Pattern[©]

CATHERINE WILKA,^a SUSAN SOLOMON,^a TIMOTHY W. CRONIN,^a DOUG KINNISON,^b AND ROLANDO GARCIA^b

^a Department of Earth, Atmospheric and Planetary Sciences, Massachusetts Institute of Technology, Cambridge, Massachusetts

^b Atmospheric Chemistry Observations and Modeling Laboratory, National Center for Atmospheric Research, Boulder, Colorado

(Manuscript received 24 January 2020, in final form 8 October 2020)

ABSTRACT: Matsuno–Gill circulations have been widely studied in tropical meteorology, but their impact on stratospheric chemistry has seldom been explicitly evaluated. This study demonstrates that, in a model nudged to reanalysis, anticyclonic Rossby wave gyres that form near the tropopause as a result of equatorially symmetric heating in the troposphere provide a dynamical mechanism to influence tropical and subtropical atmospheric chemistry during near-equinox months. The anticyclonic flow entrains extratropical air from higher latitudes into the deep tropics of both hemispheres and induces cooling in the already cold upper-troposphere/lower-stratosphere (UTLS) region. Both of these aspects of the circulation allow heterogeneous chlorine activation on sulfuric acid aerosols to proceed rapidly, primarily via the $\text{HCl} + \text{ClONO}_2$ reaction. Precipitation rates and heating rates from reanalysis are shown to be consistent with these heating and circulation response patterns in the months of interest. This study analyzes specified dynamics simulations from the Whole Atmosphere Community Climate Model (SD-WACCM) with and without tropical heterogeneous chemistry to demonstrate that these circulations influence substantially the distributions of, for example, NO_2 and ClO in the UTLS tropics and subtropics of both hemispheres. This provides a previously unrecognized dynamical influence on the spatial structures of atmospheric composition changes in the UTLS during near-equinox months.

KEYWORDS: Atmosphere; Stratospheric circulation; Transport; Halogen chemistry; Heterogeneous chemistry

1. Introduction

Matsuno (1966) studied the equatorial waves produced in response to equatorial heating in the context of a linearized, beta-plane model, successfully identifying the equatorially trapped Kelvin wave and the off-equator Rossby wave gyre responses. Gill (1980) imposed both symmetric and asymmetric heating across the equator and calculated the response of the tropical atmosphere to these idealized perturbations using linear theory. Both papers show variants of a “bull’s eye” pattern in pressure perturbations (Fig. 9 in Matsuno 1966; Fig. 1b in Gill 1980), which are now seen as indicative of the Matsuno–Gill response. While the real atmosphere is more complicated than these simplified models, and the assumptions of steady heating and time-invariance are never perfectly valid, the basic patterns have been identified in multiple dynamical studies (Jin and Hoskins 1995; Adames and Wallace 2017; Rodwell and Hoskins 2001; among others). The wind response takes the form of two Rossby cyclones in the lower troposphere and is overlain by anticyclones in the upper troposphere/lower stratosphere (UTLS), which are located to the northwest and southwest of the heating maximum, as well as an equatorially trapped Kelvin wave to the east over the Pacific, with easterly flow in the lower troposphere and westerly flow aloft. These

zonal asymmetries in the Matsuno–Gill pattern decay upward into the stratosphere, with ascent and anomalously cold air in the lower stratosphere overlying regions of deep convection and greatest tropopause heights. The dynamics of this pattern have been widely studied in the decades since its description: here we examine some of its impacts on UTLS chemistry, which result from the combination of winds and temperature anomalies.

The importance of heterogeneous chlorine activation reactions to ozone depleting chemistry has been well established for decades (Solomon et al. 1986; Solomon 1999, and references therein) and is known to be the key driver of the so-called ozone hole. Heterogeneous reactions on stratospheric aerosols convert chlorine from the reservoir species HCl and ClONO_2 to active forms that can destroy ozone in catalytic cycles. Of particular importance are the $\text{HCl} + \text{ClONO}_2 \rightarrow \text{Cl}_2 + \text{HNO}_3$, $\text{H}_2\text{O} + \text{ClONO}_2 \rightarrow \text{HOCl} + \text{HNO}_3$, and $\text{HCl} + \text{HOCl} \rightarrow \text{H}_2\text{O} + \text{Cl}_2$ reactions. Multiple factors influence the rates of these reactions, including temperature, water vapor levels, chlorine precursor levels, and aerosol surface area. The $\text{HCl} + \text{ClONO}_2$ reaction, which is in many regions the dominant source of activation, has an extremely strong inverse temperature dependence, with reaction efficiencies that decrease by six orders of magnitude between 190 and 205 K. This dependence is due to multiple factors, but below 200 K is dominated by the increasing solubility of HCl with decreasing temperature (Shi et al. 2001). The importance of these reactions has been extensively studied in the Arctic and Antarctic for decades, and in recent years there has been an increased focus on the potential for this chemistry to proceed outside the polar regions, specifically on liquid sulfuric acid aerosols that are

[©] Supplemental information related to this paper is available at the Journals Online website: <https://doi.org/10.1175/JAS-D-20-0025.s1>.

Corresponding author: Catherine Wilka, cwilka@mit.edu

ubiquitous in the lower stratosphere (Anderson et al. 2017; Robrecht et al. 2019).

Solomon et al. (2016) showed that the strong anticyclone of the East Asian summer monsoon (EASM) is capable of entraining chlorine (in the form of HCl) from higher latitudes. This chlorine enters the UTLS region above the EASM anticyclone, where temperatures are anomalously cold due to the response to convective heating (Highwood and Hoskins 1998). This combination of increased chlorine mixing ratios and cold temperatures drives chlorine activation. This work motivates us to consider additional conditions for moving chlorine into cold regions in the tropics that are difficult to describe in a zonally averaged framework, such as has often been used in the past to study meridional gradients in stratospheric chemical species. An overall goal is to contribute to a growing body of research that considers the effect of eddies and other longitudinally asymmetric features on stratospheric composition and chemistry. Identifying such features would provide an improved understanding of coupling between chemistry and transport, and a potential target for future observational campaigns in the tropical UTLS.

Matsuno–Gill tropical circulation patterns have seldom been studied in connection with stratospheric chemistry until recently. Solomon et al. (2016) was one of the first studies to investigate the response of stratospheric chlorine to equatorially asymmetric heating of this type, and this work extends that by looking at the equatorially symmetric case, which is more typically found in near-equinox months. Relative to the EASM anticyclone, the equatorially symmetric Matsuno–Gill anticyclones are somewhat weaker and situated deeper in the tropics, so they advect less chlorine from higher latitudes. However, since the tropopause temperatures in the deep tropics are lower on average than those at the latitude of the EASM anticyclone, the negative temperature perturbations from this type of Matsuno–Gill circulation nonetheless drive very swift chlorine activation. As explored below, this circulation pattern provides a pathway for chlorine activation in the deep tropics in months where activation has not previously been considered.

2. Methods

a. Rainfall data

We use NOAA's Global Precipitation Climatology Project (GPCP), version 2.3, to investigate precipitation patterns, which are a good observable proxy for heating due to latent heat release. The GPCP combines observations from rain gauge stations and soundings with satellite precipitation data to produce a $2.5^\circ \times 2.5^\circ$ resolution global product that covers land and ocean at monthly resolution from 1979 to present day (Adler et al. 2003).

b. Model

We use NCAR's Community Earth System Model with a “specified dynamics” (SD) version of the Whole Atmosphere Community Climate Model, version 4, as the atmospheric component. This model configuration is formally denoted CESM(SD-WACCM4), but throughout this paper we refer to

it simply as SD-WACCM. Below 50 km, SD-WACCM is nudged to externally specified temperature, zonal and meridional wind, and surface pressure fields from the Modern-Era Retrospective Analysis for Research and Applications (MERRA), with a relaxation time of 50 h. MERRA is a global atmospheric reanalysis beginning in 1979 and continuing through 2016 that is produced and maintained by NASA (Rienecker et al. 2011). To investigate heating rates, we present monthly means derived from the daily mean output files for each pressure level of interest for the diabatic heating.

WACCM is a high-top model with detailed gas-phase and heterogeneous chemistry schemes that include the O_x , NO_x , HO_x , ClO_x , and BrO_x reaction families. The chemistry is fully interactive, with a time step of 30 min, and the model has been extensively evaluated for use in stratospheric studies (Marsh et al. 2013; Mills et al. 2017; Froidevaux et al. 2019). About 5 pptv of very short-lived substances (VSLs) are included in the total bromine loading, but chlorine from VSLs is not included. Heterogeneous reactions on cirrus ice particles are not included. SD-WACCM has $1.9^\circ \times 2.5^\circ$ (latitude–longitude) horizontal resolution, with 88 pressure levels from the surface up to 140 km. Stratospheric sulfate aerosols are modeled as three lognormal modes and include the effect of nucleation, condensation, coagulation, and sedimentation in a micro-physics scheme described in detail in Mills et al. (2016). The background sulfur loading from volcanic eruptions is taken from a database developed by Neely and Schmidt (2016) that specifies plume injection height and the amount of sulfur injected.

We consider two different runs of SD-WACCM over four years from 2009 to 2012. In the first run, labeled Chem-Dyn-Vol, the effects of chemistry, dynamics, and volcanic eruptions are all included. This run is the standard and, in SD-WACCM, represents the best attempt to simulate the real world for those years. Note, however, that the chemical scheme in Chem-Dyn-Vol does not include water ice chemistry; the implications of this are discussed below, in section 4. The second run, labeled NoHet40NS, turns off all heterogeneous reactions involving chlorine and bromine between $40^\circ N$ and $40^\circ S$ but permits heterogeneous reactions not involving these species. Temperatures at midlatitudes are too warm to drive the heterogeneous chemistry of interest here. Comparing these two runs allows us to isolate the signature of in situ tropical heterogeneous chlorine and bromine chemistry as distinct from polar regions. We examine monthly-mean output for this study and discuss the potential influence of more transient behavior in section 4.

We focus on near-equinox months for this analysis, so the influence from summer monsoonal patterns in either hemisphere should be limited. As an example, we present results below for November 2009 (a month without a major stratospheric-impacting volcanic eruption) but note that equatorially symmetric Matsuno–Gill patterns are identified in other months as well. The impacts of these Matsuno–Gill patterns are manifested in chemical responses in low latitudes of both hemispheres, whereas responses to heating displaced from the equator, such as the EASM, are confined to the warm season hemisphere of active monsoon rainfall. We find similar results in several other near-equinox months in the 4-yr time series we looked at, including April 2009

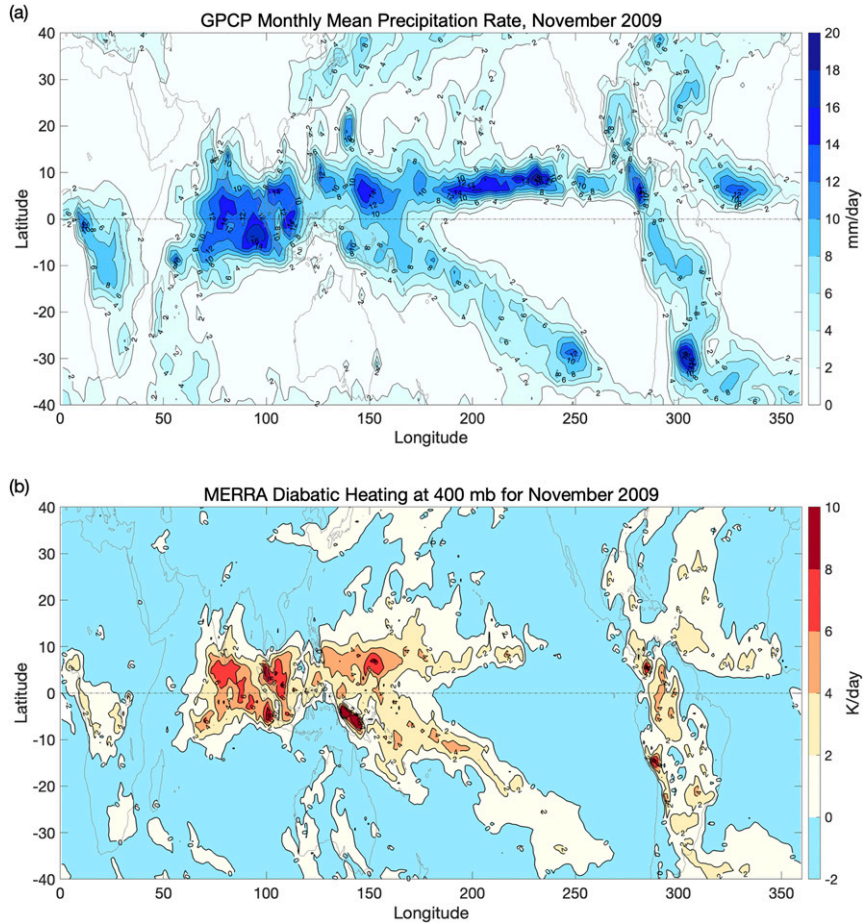


FIG. 1. (a) Precipitation (mm day^{-1}) from the GPCP and (b) diabatic heating rates (K day^{-1}) at 400 hPa from MERRA reanalysis from 40°N to 40°S, averaged for November 2009.

and 2011, November 2011, and March 2012. We expect that in a longer time series there would be many more examples.

3. Results

Figure 1a shows the mean precipitation rate for November 2009 from 40°N to 40°S from the GPCP. The highest rates occur over the equatorial Indian Ocean and over the western Pacific Ocean between 15°N and 15°S. These areas are therefore regions of strong latent heat release and are a better marker of tropical diabatic heating locations than sea surface temperature would be. We examine the diabatic heating rates at multiple levels in MERRA, which provides the meteorological fields for SD-WACCM as described above, and find that the heating tendency (K day^{-1}) due to physics is at a maximum near 400 hPa, as shown in Fig. 1b for November 2009. Although the real-world response is more varied, this resembles the vertical profile of the heating prescribed in the Gill model. The maximum in the deep tropics and the north-and-southward extending lobes track the observed precipitation patterns closely, as we would expect given the close linkage between diabatic heating rates and latent heat release. While the

heating itself extends further into the Southern Hemisphere than the Northern Hemisphere, anomalies are clearly visible in both hemispheres. These heating rates decay higher in the troposphere, and at and above the tropopause there is little remnant in the diabatic heating signal. By 100 hPa (Fig. S1 in the online supplemental material), the signal has vanished.

Figure 2a shows the vector winds and temperatures in SD-WACCM on the 85-hPa level for November 2009. The wind response to the heating pattern consists of cyclonic behavior in the lower troposphere and mirrored anticyclonic behavior in the lower stratosphere. Anticyclones can be seen in Fig. 2a on the poleward flanks of the heating pattern, specifically east of Taiwan and off the northeast coast of Australia. The eastward-propagating Kelvin wave characteristic of the Matsuno–Gill is manifested by the pattern of eastward winds visible in the equatorial Pacific east of the date line, toward the eastern part of the 192-K temperature contour. The anticyclones provide a mechanism, analogous to the anticyclone of the EASM, to entrain chlorine in reservoir form from higher latitudes. We see this when we examine SD-WACCM's November 2009 HCl distribution at 85 hPa in Fig. 2b. Higher volume mixing ratios track the anticyclone near 160°E in the Northern Hemisphere

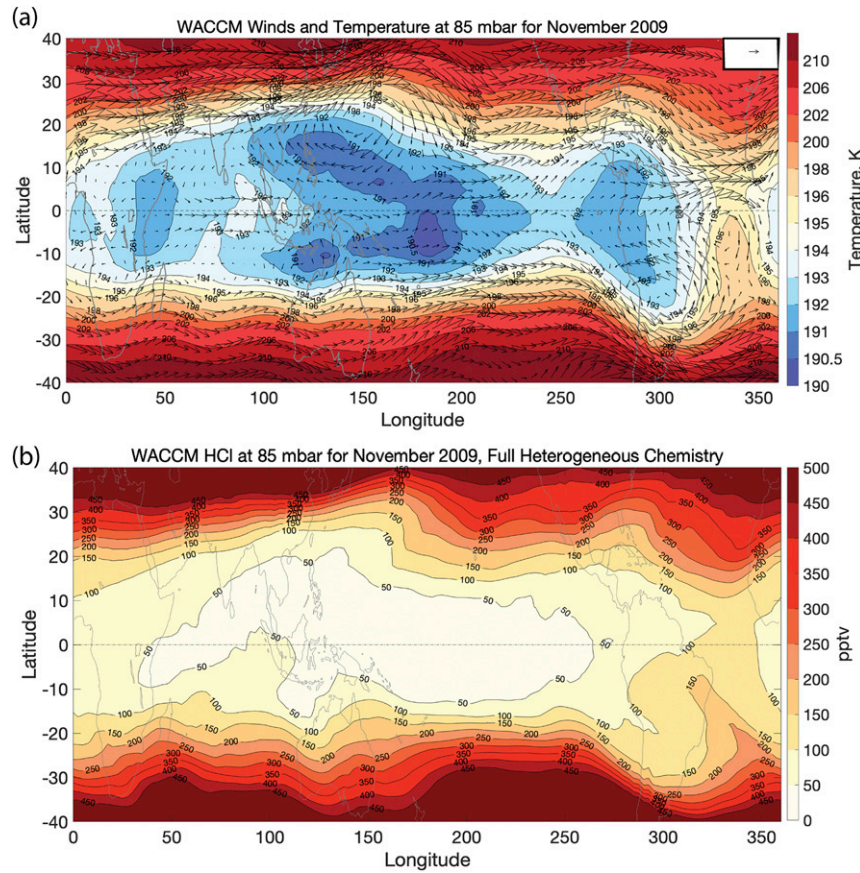


FIG. 2. (a) Monthly mean WACCM horizontal flow and temperature (K) at 85 hPa from 40°N to 40°S for November 2009. The winds are shown as vectors, with the length of the tail corresponding to the strength of the wind. A 5 m s⁻¹ vector is displayed in the upper right for scale. (b) Monthly mean WACCM HCl volume mixing ratios at 85 hPa in the tropics for November 2009. Heterogeneous chemistry is turned on at all latitudes.

and 140°E in the Southern Hemisphere, enhancing HCl by 50–100 pptv above what is seen in the rest of the Pacific Ocean at those latitudes. The other main form of reservoir chlorine, ClONO₂, is also enhanced by this effect, as can be seen in Fig. S2 in the online supplemental material.

At temperatures below 194 K, the ClONO₂ + HCl reaction proceeds extremely efficiently, whereas above 195 K the reaction rate drops so steeply that chlorine enhancement potential is minimal. We see this expected general relationship in Fig. 3, where we compare the tropics in November 2009 (Fig. 3a) to the southern high latitudes in October 2009 (Fig. 3b), when the ozone depletion in Antarctica peaks for the year. Although there is greater scatter in the tropics because some cold regions are isolated from any entrained chlorine, and the enhancement levels in Antarctica reach an order of magnitude higher, we can see that in both cases it is only possible to get enhanced ClO at colder temperatures. Temperature histories can also induce scatter: for example, air at 195 K on one day may contain chlorine activated a day or two earlier when the air was 192 K. A Lagrangian back-trajectory analysis could be used to further evaluate this question, but Fig. 3 is sufficient to

show that the highest levels of ClO are associated with temperatures below 192 K for both the Antarctic and the tropics.

The coldest temperatures (<192 K) in Fig. 2a occur over a broad region of the western Pacific and are qualitatively consistent with the concept of a stratospheric fountain first described by Newell and Gould-Stewart (1981). Highwood and Hoskins (1998) linked these stratospheric thermal anomalies to the pressure anomalies found in the upper troposphere that form part of the classic response to equatorially symmetric Matsuno–Gill heating perturbations. This circulation pattern therefore enhances chlorine activation in two ways: by entraining reservoir chlorine in the form of HCl and ClONO₂ from higher latitudes (Fig. 2b and online supplemental Fig. S2) and by lowering temperatures such that activation proceeds more rapidly (Fig. 2a). In addition to the broad region where temperatures are below 192 K, there is a smaller but still substantial region in both hemispheres where they drop below 191 K. This region is roughly symmetric about the equator, but with a greater extent in the Northern Hemisphere. There are other, smaller regions of extremely cold temperatures to the west and east of the main response pattern which may be

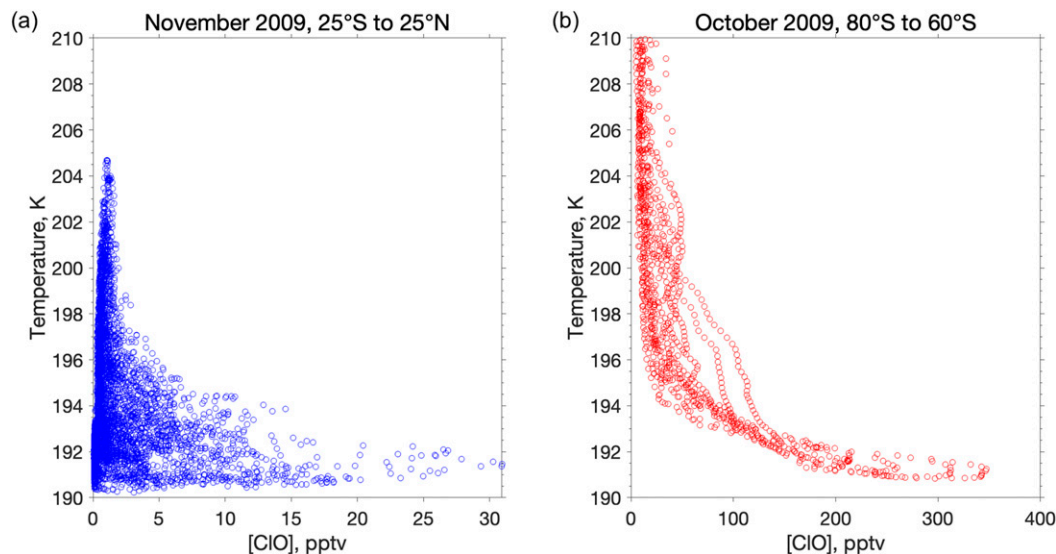


FIG. 3. Distribution of ClO mixing ratios and associated temperatures in (a) the tropics for November 2009 and (b) the Antarctic for October 2009. Both plots are at 85 hPa for all longitudes.

associated with convection over land, such as over the Amazon basin.

SD-WACCM's chemistry fields demonstrate the impacts of these cold temperatures and circulation patterns. We focus on two different chemical features at 85 hPa for November 2009: enhancement in ClO in Fig. 4a and depletion in NO₂ in Fig. 4b. As ClO is both a product of the heterogeneous reactions of interest and has very low background levels in the tropics and subtropics, it presents the clearest view of the activation response. Figure S3 in the online supplemental material compares calculations with heterogeneous chemistry turned on and off to isolate the *in situ* chemical enhancement from dynamical transport; the figure shows that heterogeneous chemistry enhances ClO from unperturbed levels of 1 pptv or less in the tropics in the absence of heterogeneous chemistry to above 25 pptv in the Northern Hemisphere lobe and above 12 pptv in the Southern Hemisphere lobe; such high levels of ClO are not normally present equatorward of about $\pm 60^\circ$ in the months in question. While ClO provides the cleanest signal for chemical activation, NO₂ is a more commonly observable species due to its higher background mixing ratios. Figure 4b shows the expected response in NO₂, of opposite sign to that of ClO, due to the recombination of NO₂ with ClO and subsequent conversion to HNO₃. It is especially illuminating to note how the pattern of chlorine activation curls around with the winds of the anticyclones. In the Southern Hemisphere in particular, there is a marked decrease in activation near the center of the anticyclone off the northeast coast of Australia. We see continued but decreasing elevated levels in a west–east band across the Pacific. Examination of the reaction rates of the three main heterogeneous chlorine activation reactions described above ($\text{HCl} + \text{ClONO}_2 \rightarrow \text{Cl}_2 + \text{HNO}_3$, $\text{H}_2\text{O} + \text{ClONO}_2 \rightarrow \text{HOCl} + \text{HNO}_3$, and $\text{HCl} + \text{HOCl} \rightarrow \text{H}_2\text{O} + \text{Cl}_2$) in Fig. S4 in the online supplemental material confirms that the *in situ* activation is driven by a combination of available

chlorine and cold temperatures, with the former limiting activation on the equatorward side and the latter limiting it on the poleward side. Both ClO and NO₂ changes span somewhat larger regions than the chemical rates; this is likely associated with advection by the equatorward edges of the subtropical jets or the Kelvin wave part of the Matsuno–Gill wind response. NO₂ changes show a broader pattern than ClO, reflecting the former's longer lifetime in the stratosphere and thus ability to be carried by the circulation. There is more activation in the Northern Hemisphere than in the Southern Hemisphere, consistent with the more extensive region of cold temperatures there. It is notable that there is little enhancement of chlorine activation over the equator proper despite the cold temperatures, as the meridional transport of chlorine from higher latitudes weakens dramatically there, in accordance with the Matsuno–Gill meridional wind response vanishing at the equator for symmetric heating.

Although the longitudinally resolved plots give the clearest demonstration of the implications of a Matsuno–Gill type flow for stratospheric chemistry, this activation signal can also be seen in the zonal mean in both ClO and NO₂. Figures 5a and 5b show the ClO and NO₂ mixing ratios for November 2009 at 85 hPa for the Chem-Dyn-Vol run and the NoHet40NS run. A partial zonal mean from 100° to 250°E emphasizes the region of interest while excluding the influence of the continental landmasses, but the same features are present in the full zonal mean (Fig. S5 in the online supplemental material) despite dilution from chemically quiescent longitudes. ClO shows an extremely clear dual hemisphere enhancement, stronger in the Northern Hemisphere, with background levels nearly zero in the absence of heterogeneous chemistry. NO₂ has a more pronounced hemispheric asymmetry, although the signal is present in both. The feature in NO₂ near 10°N is especially significant, as the Chem-Dyn-Vol mixing ratio of ~ 60 pptv, compared to the NoHet40NS concentration of ~ 200 pptv, should be observable.

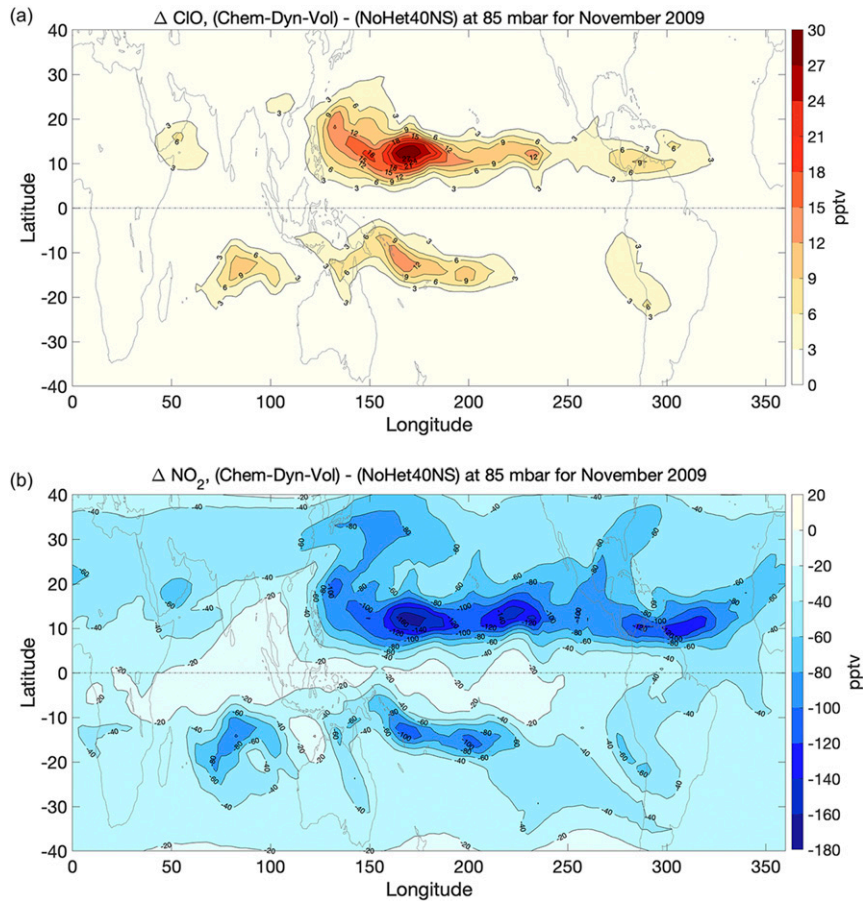


FIG. 4. Differences in the monthly mean distribution of (a) ClO and (b) NO₂ at 85 hPa in SD-WACCM between the runs with and without heterogeneous chlorine and bromine chemistry turned on in the tropics. Red values indicate relative enhancement, and blue values indicate relative depletion.

Perturbations are even larger at some longitudes as shown in Fig. 4.

4. Discussion

We find clear signals of enhancement in ClO and depletion in NO₂ in SD-WACCM in the tropical lower stratosphere in months near the equinoxes due to the presence of heterogeneous chemistry on liquid sulfuric acid aerosols. We present results from November 2009 and find similar patterns in several other months as well, as shown in the ClO differences over the entire time series (Fig. S6 in the online supplemental material). In particular, November 2011 (Fig. S6d), December 2011 (Fig. S6a), April 2009 (Fig. S6b), and April 2011 (Fig. S6b) show double bull's-eyes. Boreal summer (Fig. S6c) and austral summer (Fig. S6a) are both dominated by single-hemisphere enhancements associated with their monsoons. The strong East Asian summer monsoon anticyclone leads to the largest chlorine enhancement of these asymmetric heating responses, supporting what was previously found in [Solomon et al. \(2016\)](#). It is worth noting that, while November 2010–January 2011

have very high enhancement, the Merapi volcano erupted at the end of October 2010, increasing the aerosol surface areas and heterogeneous reaction rates, and likely dominates the signal for months.

We have systematically traced the chlorine activation back to the effects of a Matsuno–Gill circulation pattern caused by diabatic heating in equatorial regions of the western Pacific. This circulation pattern includes anticyclones in the lower stratosphere of both hemispheres that entrain chlorine to lower latitudes, as well as very cold lower-stratospheric temperatures overlying regions where the tropopause is high. Winds and temperatures combine to drive efficient heterogeneous chlorine activation. The changes in ClO and NO₂ background mixing ratios provide a testable signature of this mechanism that should be visible to future measurement campaigns in the region, particularly using airborne instruments. Unfortunately, the current generation of chemistry-focused satellites does not measure ClO in the tropical UTLS, but, should that change, this pattern should also be visible on a large scale as seen in the model. While the differences between the SD-WACCM runs we present successfully isolate the signal of chlorine activation

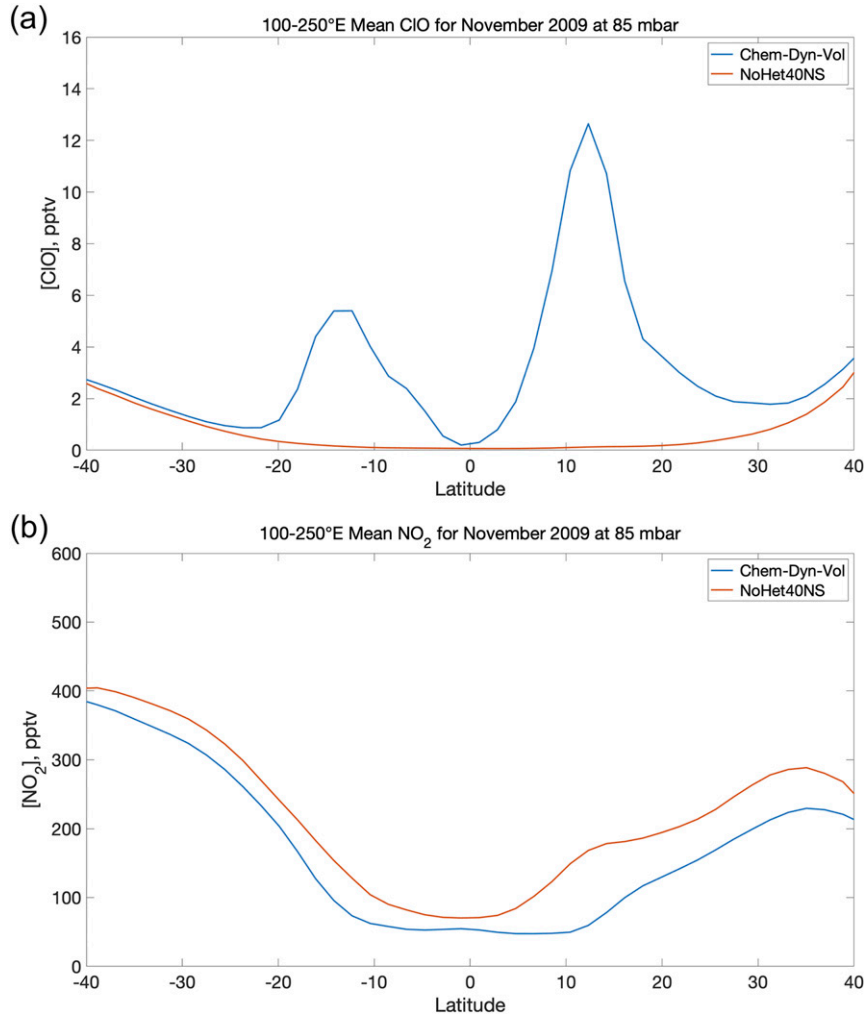


FIG. 5. Monthly longitudinal means from 100° to 250°E for (a) ClO and (b) NO₂ in SD-WACCM at 85 hPa from 40°S to 40°N for November 2009. The blue line is the Chem-Dyn-Vol run with full heterogeneous chemistry turned on, and the red line is the NoHet40NS run with heterogeneous chlorine and bromine chemistry turned off in the tropics.

due to heterogeneous reactions, the underlying meteorological fields and thus the Matsuno–Gill circulations are the same for all runs. To quantify the importance of these for transporting chlorine, runs with modified dynamics that suppress the Matsuno–Gill response would be required. While such comparisons are beyond the scope of the present study, they could be a useful component of future ones.

Although the years we look at in this study were devoid of major volcanic eruptions, in the past decade numerous studies have shown that aerosols from the more frequent, moderate-sized volcanoes have a discernible impact on many aspects of stratospheric chemistry (Solomon et al. 2011; Naik et al. 2017; Adams et al. 2017; Wilka et al. 2018). Sarychev Peak erupted in June 2009 and lofted measurable sulfur to the stratosphere, so November 2009 was not “volcanically clean.” Nor was 2011, due to the Nabro eruption in June of that year. However, as volcanically clean years seem to be more the exception than

the rule (Mills et al. 2016; Vernier et al. 2011), at least in recent decades, 2009 may be a fairly typical year in terms of tropical sulfate levels.

The model chemistry relies on several assumptions about heterogeneous chemistry whose validity could impact our results. The parameterized heterogeneous activation rates are based on laboratory studies that contain few direct measurements at the coldest temperatures and have not been updated for almost two decades. Furthermore, these studies assumed pure liquid H₂O/H₂SO₄ mixtures, so that the effects of freezing and of any doping with pollutant nitrates or organics are poorly constrained. The extent to which these matter in the real world depends on both the aerosol composition of the tropical lower stratosphere and the degree to which sulfates are internally versus externally mixed with other species. The degree of accuracy with which models capture relevant stratospheric aerosol processes and composition changes is an area of active research

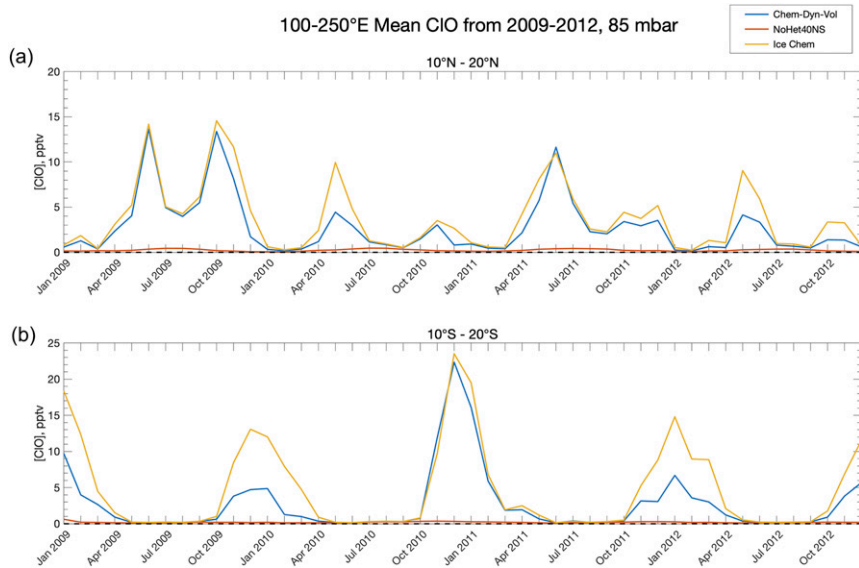


FIG. 6. Time series of monthly mean CIO over the Pacific Ocean in the (a) Northern Hemisphere and (b) Southern Hemisphere tropics. Latitude bands are chosen to maximize the activation signal and isolate interhemispheric differences. The blue line is the Chem-Dyn-Vol run with full heterogeneous chemistry turned on but no ice chemistry, the red line is the NoHet40NS run with heterogeneous chlorine and bromine chemistry turned off in the tropics, and the yellow line is the Ice Chem run with full heterogeneous chemistry and an additional ice chemistry parameterization included.

(Kremser et al. 2016, and references therein). One recent study (Höpfner et al. 2019) found elevated levels of solid ammonium nitrate in the upper troposphere during the Asian summer monsoon due to convective uplift of NH_3 . However, they did not find elevated ammonium nitrate outside of the summer monsoon months, that is, for the months of interest here. Further, sulfate aerosols can be expected to be dominant in volcanically perturbed periods.

While the version of SD-WACCM we use does not account for heterogeneous chemistry on cirrus ice cloud particles, we expect such reactions to enhance our modeled activation. Cirrus chemistry parameterizations are subject to large uncertainties, but we test our expectation by running SD-WACCM with an ice chemistry parameterization implemented for the four years of interest and plot the CIO mixing ratios in Fig. 6 along with the Chem-Dyn-Vol and NoHet40NS runs for the same Pacific region of interest as Fig. 5. We see in Fig. 6 that ice chemistry increases activation, as expected, but the magnitude of its impact varies greatly both among years and between hemispheres. For November 2009, ice chemistry appears to enhance CIO more in the Southern Hemisphere (Fig. 6b) than the Northern Hemisphere (Fig. 6a), but in November 2010 there is little effect in either hemisphere. The relative importance of cirrus clouds is an ongoing area of study, but it is important to note that the enhancements seen in Fig. 6, regardless of season, occur in addition to activation caused by liquid sulfuric acid aerosols, and we do not see any significant enhancements in the absence of liquid sulfuric acid aerosol-driven activation. Thus, we feel confident that our results capture the main features of chlorine activation in the tropical UTLS, even without considering cirrus input.

An additional source of uncertainty in the model results comes from the adopted temperature profiles. MERRA temperatures near the tropopause, to which SD-WACCM is relaxed, assimilate both satellite and in situ observations, so we expect that they capture the mean structure well. However, the number of levels in the UTLS is relatively small, and may fail to capture some of the variance in temperature structure often seen in higher vertical resolution radiosondes, especially due to situations such as a double-peaked cold point tropopause or small-scale wave activity. We recognize that this smoothing of the temperature structure will mute some of the corresponding vertical structure in the chemistry, and in particular may underestimate activation if the cold point occurs between model levels. This is an active area for further research and the importance of temperature resolution for chemistry could inform considerations of future subgrid-scale modeling parameterizations, as well as be a target of investigation for higher-resolution models.

Another promising direction for further exploration is the role that wave activity on different time scales has on the likelihood and lifetime of the patterns that we investigate here. Tropical winds, temperatures, and resultant chemistry patterns are influenced from year to year by El Niño–Southern Oscillation and the quasi-biennial oscillation, and on subseasonal time scales by the Madden–Julian oscillation (MJO) and mixing from mid-latitude eddies. As we have examined only a monthly-mean response, we recognize that on shorter time scales the activation could be both stronger and more localized. This is especially likely in the case of modulation of convection by the MJO, which varies in location over its cycle and in strength between different events.

While it is intriguing that 2009 and 2011 both seem to display more activation in fall and spring (Fig. S6 in the online supplemental material), the current study does not span enough years to determine what dynamical phases or combinations thereof are most responsible for influencing chemistry. A systematic investigation of a longer time series could also help quantify the influence of summer monsoonal circulations of varying strength on this chemistry. Quantifying how both the background state of the atmosphere and the activity of more transient phenomena influence the likelihood of finding these patterns is an area of ongoing investigation.

5. Conclusions

This study has expanded our knowledge of where heterogeneous chlorine activation chemistry can take place in months near the equinoxes and has revealed new connections between tropical meteorology and stratospheric chemistry. The ClO and NO₂ levels that we have modeled provide observable targets for future aircraft campaigns or satellites focused on the tropical UTLS. For example, measurements of the anomalies seen in both hemispheres (as in Fig. 4) would serve as a characteristic signature of the response as described here. Such campaigns could also use this chemistry to deepen our understanding of the stratospheric equatorially symmetric Matsuno–Gill circulation and transport patterns, with chemical enhancements providing observable indicators for dynamical studies.

Furthermore, while we have focused on the heterogeneous chlorine reactions most relevant for ozone depletion in this region, it is notable that other chemical constituents and processes will also be affected. For example, all reactants with a steep equator-to-pole concentration gradient are expected to be affected by the Matsuno–Gill wind pattern described here. Reactions with a sufficiently strong temperature sensitivity will also be influenced. For both chlorine-dependent and other reactions, continuing to investigate the impacts of zonally asymmetric circulation patterns on atmospheric chemistry is an area that is ripe for further research.

Acknowledgments. We acknowledge high-performance computing support from Cheyenne ([doi:10.5065/D6RX99HX](https://doi.org/10.5065/D6RX99HX)) provided by NCAR's Computational and Information Systems Laboratory, sponsored by the National Science Foundation. Authors Wilka, Solomon, and Cronin are grateful for partial support under NSF Grant 1906719 from the Atmospheric Chemistry division. Author Kinnison is grateful for partial support under NASA ACMAP Grant 80NSSC19K0952. The National Center for Atmospheric Research is sponsored by the National Science Foundation.

Data availability statement. We thank NOAA's Earth System Research Laboratory for the GCPC rainfall data (available freely online at esrl.noaa.gov/psd/data/gridded/data.gcpc.html). We thank NASA Goddard Space Flight Center for the MERRA data (available freely online at <http://disc.sci.gsfc.nasa.gov/>). WACCM is a component of the Community Earth System Model (CESM), which is supported

by the National Science Foundation. WACCM runs are available online (https://acomstaff.acom.ucar.edu/dkin/JAS_Wilka_2020/).

REFERENCES

Adames, Á. F., and J. M. Wallace, 2017: On the tropical atmospheric signature of El Niño. *J. Atmos. Sci.*, **74**, 1923–1939, <https://doi.org/10.1175/JAS-D-16-0309.1>.

Adams, C., A. E. Bourassa, C. A. McLinden, C. E. Sioris, T. von Clarmann, B. Funke, L. A. Rieger, and D. A. Degenstein, 2017: Effect of volcanic aerosol on stratospheric NO₂ and N₂O₅ from 2002–2014 as measured by Odin-OSIRIS and Envisat-MIPAS. *Atmos. Chem. Phys.*, **17**, 8063–8080, <https://doi.org/10.5194/acp-17-8063-2017>.

Adler, R. F., and Coauthors, 2003: The version-2 Global Precipitation Climatology Project (GPCP) monthly precipitation analysis (1979–present). *J. Hydrometeor.*, **4**, 1147–1167, [https://doi.org/10.1175/1525-7541\(2003\)004<1147:TVGPCP>2.0.CO;2](https://doi.org/10.1175/1525-7541(2003)004<1147:TVGPCP>2.0.CO;2).

Anderson, J. G., and Coauthors, 2017: Stratospheric ozone over the United States in summer linked to observations of convection and temperature via chlorine and bromine catalysis. *Proc. Natl. Acad. Sci. USA*, **114**, E4905–E4913, <https://doi.org/10.1073/pnas.1619318114>.

Froidevaux, L., D. E. Kinnison, R. Wang, J. Anderson, and R. A. Fuller, 2019: Evaluation of CESM1 (WACCM) free-running and specified dynamics atmospheric composition simulations using global multispecies satellite data records. *Atmos. Chem. Phys.*, **19**, 4783–4821, <https://doi.org/10.5194/acp-19-4783-2019>.

Gill, A. E., 1980: Some simple solutions for heat-induced tropical circulation. *Quart. J. Roy. Meteor. Soc.*, **106**, 447–462, <https://doi.org/10.1002/qj.49710644905>.

Highwood, E. J., and B. J. Hoskins, 1998: The tropical tropopause. *Quart. J. Roy. Meteor. Soc.*, **124**, 1579–1604, <https://doi.org/10.1002/qj.49712454911>.

Höpfner, M., and Coauthors, 2019: Ammonium nitrate particles formed in upper troposphere from ground ammonia sources during Asian monsoons. *Nat. Geosci.*, **12**, 608–612, <https://doi.org/10.1038/s41561-019-0385-8>.

Jin, F., and B. J. Hoskins, 1995: The direct response to tropical heating in a baroclinic atmosphere. *J. Atmos. Sci.*, **52**, 307–319, [https://doi.org/10.1175/1520-0469\(1995\)052<0307:TDRTTH>2.0.CO;2](https://doi.org/10.1175/1520-0469(1995)052<0307:TDRTTH>2.0.CO;2).

Kremser, S., and Coauthors, 2016: Stratospheric aerosol—Observations, processes, and impact on climate. *Rev. Geophys.*, **54**, 278–335, <https://doi.org/10.1002/2015RG000511>.

Marsh, D. R., M. J. Mills, D. E. Kinnison, J. F. Lamarque, N. Calvo, and L. M. Polvani, 2013: Climate change from 1850 to 2005 simulated in CESM1 (WACCM). *J. Climate*, **26**, 7372–7391, <https://doi.org/10.1175/JCLI-D-12-00558.1>.

Matsuno, T., 1966: Quasi-geostrophic motions in the equatorial area. *J. Meteor. Soc. Japan*, **44**, 25–43, https://doi.org/10.2151/jmsj1965.44.1_25.

Mills, M. J., and Coauthors, 2016: Global volcanic aerosol properties derived from emissions, 1990–2014, using CESM1 (WACCM). *J. Geophys. Res. Atmos.*, **121**, 2332–2348, <https://doi.org/10.1002/2015JD024290>.

—, and Coauthors, 2017: Radiative and chemical response to interactive stratospheric sulfate aerosols in fully coupled CESM1 (WACCM). *J. Geophys. Res. Atmos.*, **122**, 13 061–13 078, <https://doi.org/10.1002/2017JD027006>.

Naik, V., L. W. Horowitz, M. Daniel Schwarzkopf, and M. Lin, 2017: Impact of volcanic aerosols on stratospheric ozone recovery. *J. Geophys. Res. Atmos.*, **122**, 9515–9528, <https://doi.org/10.1002/2016JD025808>.

Neely, R., and A. Schmidt, 2016: VolcanEESM: Global volcanic sulphur dioxide (SO_2) emissions database from 1850 to present, version 1.0. Centre for Environmental Data Analysis, accessed 30 December 2015, <https://doi.org/10.5285/76ebdc0b-0eed-4f70-b89e-55e606bcd568>.

Newell, R. E., and S. Gould-Stewart, 1981: A stratospheric fountain? *J. Atmos. Sci.*, **38**, 2789–2796, [https://doi.org/10.1175/1520-0469\(1981\)038<2789:ASF>2.0.CO;2](https://doi.org/10.1175/1520-0469(1981)038<2789:ASF>2.0.CO;2).

Rienecker, M. M., and Coauthors, 2011: MERRA: NASA's Modern-Era Retrospective Analysis for Research and Applications. *J. Climate*, **24**, 3624–3648, <https://doi.org/10.1175/JCLI-D-11-00015.1>.

Robrecht, S., and Coauthors, 2019: Mechanism of ozone loss under enhanced water vapour conditions in the mid-latitude lower stratosphere in summer. *Atmos. Chem. Phys.*, **19**, 5805–5833, <https://doi.org/10.5194/acp-19-5805-2019>.

Rodwell, M. J., and B. J. Hoskins, 2001: Subtropical anticyclones and summer monsoons. *J. Climate*, **14**, 3192–3211, [https://doi.org/10.1175/1520-0442\(2001\)014<3192:SAASM>2.0.CO;2](https://doi.org/10.1175/1520-0442(2001)014<3192:SAASM>2.0.CO;2).

Shi, Q., J. T. Jayne, C. E. Kolb, D. R. Worsnop, and P. Davidovits, 2001: Kinetic model for reaction of ClONO_2 with H_2O and HCl and HOCl with HCl in sulfuric acid solutions. *J. Geophys. Res.*, **106**, 24 259–24–274, <https://doi.org/10.1029/2000JD000181>.

Solomon, S., 1999: Stratospheric ozone depletion: A review of concepts and history. *Rev. Geophys.*, **37**, 275–316, <https://doi.org/10.1029/1999RG900008>.

—, R. R. Garcia, F. S. Rowland, and D. J. Wuebbles, 1986: On the depletion of Antarctic ozone. *Nature*, **321**, 755–758, <https://doi.org/10.1038/321755a0>.

—, J. S. Daniel, R. R. Neely, J. P. Vernier, E. G. Dutton, and L. W. Thomason, 2011: The persistently variable “background” stratospheric aerosol layer and global climate change. *Science*, **333**, 866–870, <https://doi.org/10.1126/science.1206027>.

—, and Coauthors, 2016: Monsoon circulations and tropical heterogeneous chlorine chemistry in the stratosphere. *Geophys. Res. Lett.*, **43**, 12 624–12 633, <https://doi.org/10.1002/2016GL071778>.

Vernier, J. P., and Coauthors, 2011: Major influence of tropical volcanic eruptions on the stratospheric aerosol layer during the last decade. *Geophys. Res. Lett.*, **38**, L12807, <https://doi.org/10.1029/2011GL047563>.

Wilka, C., K. Shah, K. Stone, S. Solomon, D. Kinnison, M. Mills, A. Schmidt, and R. R. Neely, 2018: On the role of heterogeneous chemistry in ozone depletion and recovery. *Geophys. Res. Lett.*, **45**, 7835–7842, <https://doi.org/10.1029/2018GL078596>.